

②

AD-A143 225

# NAVAL POSTGRADUATE SCHOOL

Monterey, California



TIME DEVELOPMENT OF  
CERENKOV RADIATION

Fred R. Buskirk and John R. Neighbours

May 1984

Technical Report

DTIC FILE COPY

Approved for public release; distribution unlimited

Prepared for:  
Naval Sea Systems Command  
WASHINGTON, DC 20362

JUL 20 1984

84 7 20 071

E

NAVAL POSTGRADUATE SCHOOL  
Monterey, California

Commodore R. H. Shumaker  
Superintendent

David Schrady  
Provost

The work reported herein was supported by the Naval  
Sea Systems Command.

Reproduction of all or part of this report is authorized.

This report was prepared by:

*Fred R Buskirk*

F. R. Buskirk  
Professor of Physics

*John R Neighours*

J. R. Neighours  
Professor of Physics

Reviewed by:

Released by:

*G. E. Schacher*

G. E. Schacher, Chairman  
Department of Physics

*V. T. Marshall*  
for J. N. Dyer

Dean of Science and Engineering

UNCLASSIFIED

SECURITY CLASSIFICATION OF THIS PAGE (When Data Entered)

REPORT DOCUMENTATION PAGE		READ INSTRUCTIONS BEFORE COMPLETING FORM
1. REPORT NUMBER NPS-61-84-006	2. GOVT ACCESSION NO. AD-A143225	3. RECIPIENT'S CATALOG NUMBER
4. TITLE (and Subtitle) Time Development of Cerenkov Radiation		5. TYPE OF REPORT & PERIOD COVERED Technical Report
7. AUTHOR(s) Fred R. Buskirk John R. Neighbours		6. PERFORMING ORG. REPORT NUMBER
9. PERFORMING ORGANIZATION NAME AND ADDRESS Naval Postgraduate School Monterey, California 93943		10. PROGRAM ELEMENT, PROJECT, TASK AREA & WORK UNIT NUMBERS 62768N N000248/WR10821
11. CONTROLLING OFFICE NAME AND ADDRESS Naval Sea Systems Command PMS405		12. REPORT DATE May 1984
14. MONITORING AGENCY NAME & ADDRESS (if different from Controlling Office)		13. NUMBER OF PAGES
		15. SECURITY CLASS. (of this report) Unclassified
		15a. DECLASSIFICATION/DOWNGRADING SCHEDULE
16. DISTRIBUTION STATEMENT (of this Report) Approved		
17. DISTRIBUTION STATEMENT (of the abstract entered in Block 20, if different from Report)		
18. SUPPLEMENTARY NOTES		
19. KEY WORDS (Continue on reverse side if necessary and identify by block number) Cerenkov Radiation Relativistic electron beams Radiation Field		
20. ABSTRACT (Continue on reverse side if necessary and identify by block number) See attached		

DD FORM 1473  
1 JAN 73EDITION OF 1 NOV 65 IS OBSOLETE  
S/N 0102-LF-014-6601

UNCLASSIFIED

SECURITY CLASSIFICATION OF THIS PAGE (When Data Entered)

# TIME DEVELOPMENT OF CERENKOV RADIATION

Fred R. Buskirk

John R. Neighbours

Physics Department  
Naval Postgraduate School  
Monterey, California 93943

## ABSTRACT

Most developments of Cerenkov Radiation are in terms of the Fourier components of the fields and power emitted by a single electron. When many electrons in a compact bunch are emitted from an accelerator, the bunch radiates coherently and at a lower frequency than for a single electron. The theory for the time structure of the fields arising from a charge bunch is developed, and it is shown that the source of the radiation is  $di/dt$ . Present detector technology should be able to resolve these fields.

Accession For	
NTIS GRA&I	<input checked="" type="checkbox"/>
DTIC TAB	<input type="checkbox"/>
Unannounced	<input type="checkbox"/>
Justification	
By _____	
Distribution/	
Availability Codes	
Dist	Avail and/or Special
A-1	



- A -

## TIME DEVELOPMENT OF CERENKOV RADIATION

### INTRODUCTION

Cerenkov radiation, produced by a charge or group of charges, moving faster than the speed of electromagnetic radiation in a medium, has been investigated, starting with the experiments of Cerenkov<sup>1</sup> in 1934 and the explanation by Frank and Tamm<sup>2</sup> in 1937. Since power radiated by a single charged particle is proportional to the frequency, most of the research effort has been devoted to the relatively intense optical radiation which is favored over the microwave region by a factor of about  $10^4$ . The optical results<sup>3,4</sup> are given in terms of the Fourier components of the fields and the radiated power.

In our previous work<sup>5,6</sup> it was noted that microwave radiation can be significant because all the electrons in an accelerator bunch (about  $10^9$ ) radiate coherently; an effect which more than offsets the single particle increase in radiated power with frequency. For an electron beam generated by a traveling wave Linac and passing through air, it was shown that the various harmonics of the basic frequency up to about the tenth are emitted. (In the case of an L or S band Linac, these correspond to 10 GHz and 30 GHz respectively.)

The time structure of Cerenkov radiation fields in the optical and even in the higher frequency microwave regions is difficult to observe because the detectors register power. One of the few

treatments of the time dependence, by Tamm<sup>7</sup> in 1939, showed that the optical radiation by an electron is singular on the Cerenkov front. Here we consider the time structure of fields generated when electron bunches radiate coherently; in a development which complements the frequency domain analysis of our earlier work<sup>5,6</sup>.

The fields should be observable for beams from induction accelerators which produce bunches much longer than those produced by S or L band Linacs.

## MAGNETIC RADIATION FIELD

The purpose of this paper is to present a development of the time dependence of the electric field generated by the Cerenkov mechanism. The method is first to determine the potentials from the moving charge distribution, and subsequently to obtain the fields (in cgs units) from the potentials by

$$\vec{B} = \nabla \times \vec{A} \quad (1)$$

$$\vec{E} = -\nabla\phi - \frac{1}{c_0} \frac{\partial \vec{A}}{\partial t} \quad (2)$$

We assume a charge density function  $\rho_v$  and a current density  $\vec{j}_v = \rho_v \vec{v}/c_0$  with the velocity  $\vec{v}$  in the plus  $z$  direction. The charge and current are assumed to be concentrated along the  $z$  axis such that

$$\rho_v(\vec{r}, t) = \rho(z, t) \delta(x) \delta(y) \quad (3)$$

and the charge is assumed to move with no change in shape so that the  $z$  and  $t$  dependence of the charge is

$$\rho(z, t) = \rho_0(z-vt) \quad (4)$$

Note that  $\rho_v$  and  $\vec{j}_v$  represent the usual charge and current densities, while  $\rho$  and  $\rho_0$  throughout this paper are charge per unit length. The velocity of light is  $c$  and  $c_0$  in the medium and free space, respectively.

The potentials are found by taking the usual retarded solutions to the wave equations; which become under the assumption of a line distribution of charge (3),

$$\phi(\vec{r}, t) = \epsilon^{-1} \int R^{-1} \rho(\vec{r}', t') dz' \quad (5)$$

$$\vec{A}(\vec{r}, t) = \frac{\vec{v}}{c_0} \int R^{-1} \rho(\vec{r}', t') dz' \quad (6)$$

where  $\vec{R} = \vec{r} - \vec{r}'$  and  $t'$  is the retarded time

$$t' = t - |\vec{r} - \vec{r}'|/c$$

Now (4), the assumption of rigid motion of the charge distribution, can be incorporated into the potentials, and a new variable  $u(z') = z' - vt'$  can be introduced so that the potentials (5) and (6) become

$$\phi(\vec{r}, t) = \epsilon^{-1} \int R^{-1} \rho_0(u) dz' \quad (8)$$

$$\vec{A}(\vec{r}, t) = \frac{\vec{v}}{c_0} \int R^{-1} \rho_0(u) dz' \quad (9)$$

Also, since the charge is confined to the  $z'$  axis, the new variable  $u(z')$  can be written more explicitly.

$$u(z') = z' - vt + \frac{v}{c} [x^2 + y^2 + (z - z')^2]^{1/2} \quad (10)$$



The magnetic field  $\vec{B}$  may be calculated from (1) and since  $\vec{A}$  has only a z-component,  $\vec{B}$  has only the x and y components,  
 $B_x = \frac{\partial}{\partial y} A_z$  and  $B_y = -\frac{\partial}{\partial x} A_z$ . Carrying out the differentiation for the x component gives

$$B_x = \frac{v}{c_0} \int \frac{\partial}{\partial y} R^{-1} \rho_0(u) dz' \quad (11)$$

$$+ \frac{v}{c_0} \int R^{-1} \frac{\partial}{\partial y} \rho_0(u) dz'$$

For radiation, the first integral, falling off as  $R^{-2}$  at large distances, will be neglected and only the second term will be considered further. From (10), it is seen that  $u$  is a function of  $x$  and  $y$  so that the second integral can be written

$$B_x = \frac{v^2}{cc_0} \int \frac{y}{R^2} \rho_0'(u) dz' \quad (12)$$

where  $\rho_0'(u)$  is the derivative of  $\rho_0$  with respect to its argument  $u$ . The corresponding expression for  $B_y$  has  $y$  replaced by  $(-x)$ . These two components can be combined to give the total magnetic radiation field  $\vec{B}$ . In the cylindrical coordinates,  $(s, \theta, z)$  where  $s$  is the radius vector  $s = (x^2 + y^2)^{1/2}$ ,  $\vec{B}$  is tangential (i.e. in the  $\hat{\theta}$  direction) with a magnitude given by

$$B = \frac{v^2}{cc_0} \int \frac{s}{R^2} \rho_0'(u) dz' \quad (13)$$

### TIME DEVELOPMENT

In order to evaluate (13) for B, it is necessary to consider the dependence of  $u$  on  $z'$  as given in (10). In the  $u$ - $z'$  plane, the first two terms are a straight line with unit slope and an intercept which changes with time, while the third term is a hyperbola opening in the  $+u$  direction with asymptotic slopes of  $\pm \frac{v}{c}$ . The sum of these two curves is  $u(z')$ . In the Cerenkov case with  $v > c$ , the result is a curve whose ends both point upward as shown in Fig. 1. As time increases, the entire curve will translate downward to smaller  $u$  values as a result of the negative second term in (10).

Only changing currents (those with a non zero  $\rho_0'$ ) will contribute to the magnetic radiation field (13). To proceed and demonstrate the method, a ramp-front current pulse is chosen as a simple example. Assuming that the front end of a current pulse increases linearly up to a constant value, the derivative  $\rho_0'(u)$  will be a constant valued square pulse of magnitude  $\rho_m'$  as is also shown in Fig. 1. The corresponding negative  $\rho_0'(u)$  pulse occurring at the tail of a current pulse is not shown and its effect is considered separately.

For large negative times, the  $u(z')$  curve (a) is completely above the pulse-like non zero portion of the  $\rho_0'(u)$  curve so that the contribution in (13) to B from  $\rho_0'(u)$  is zero and therefore, B is zero. As time increases, the  $u(z')$  curve moves downward until the B pulse begins when  $u(z')$  is tangent (curve b) to the upper portion of the  $\rho_0'(u)$  pulse. The value

of the integral in (13) increases as  $u(z)$  continues its constant downward motion with increasing time until  $u(z')$  becomes tangent (curve 3) with the lower part of the  $\rho_0'(u)$  pulse. At this time the non zero part of the integral has the largest extent -from  $z_1$  to  $z_2$ . At later times, the integral breaks into two regions of the  $z'$  axis and if  $\rho_0'(u)$  is constant, the value of the integral decreases with increasing time because the extent of the integral in the two regions continues to decrease as a result of the upward turn of  $u(z')$ .

This calculation may be carried further to determine the time structure (shape) of the resulting B pulse. Although the expression (13) for B can be integrated directly in the case where the slope  $\rho_0'(u)$  is constant, it is instructive to carry out the calculation by developing  $u$  in a power series. Denoting  $z_0'$  as the value of  $z'$  at which  $u(z')$  has zero slope, the values of  $z_0'$ ,  $u(z_0')$  and the second derivative are

$$z_0' = -s \left( \frac{v^2}{c^2} - 1 \right)^{-1/2} \quad (14)$$

$$u(z_0') = s \left( \frac{v^2}{c^2} - 1 \right)^{-1/2} - vt \quad (15)$$

$$\left. \frac{\partial^2 u}{\partial z'^2} \right|_{z_0} = \frac{1}{s} \frac{c^2}{v^2} \left( \frac{v^2}{c^2} - 1 \right)^{3/2} \equiv 2A \quad (16)$$

so that  $u$  can be expressed as a power series about the minimum

$$u = u(z_0') + A(z' - z_0')^2 \quad (17)$$

The limits  $z_1'$  and  $z_2'$  can be written in terms of the minimum value as  $z_2' = z_0' + \Delta z$  and  $z_1' = z_0' - \Delta z'$  where  $\Delta z'$  is the value of  $z' - z_0'$  such that the difference  $u(z') - u(z_0') = a$ , the width of the current derivative pulse  $\rho_0'$ . Then from (17),  $a = A(\Delta z')^2$  or

$$\Delta z' = (a/A)^{1/2} \quad (18)$$

Using this value, the maximum magnetic radiation field for the rising front of the magnetic field pulse is easily evaluated from (13) under the assumption that  $s$  and  $R$  are slowly varying to give

$$B_{\max} = \frac{v^2}{cc_0} \frac{s}{R^2} \rho_m' \quad 2 \left( \frac{a}{A} \right)^{1/2} \quad (19)$$

Values of  $B$  for the rise up to the peak value given above are found by the same process but using appropriately smaller values of  $\Delta z'$ . The result is that the integral (and therefore  $B$ ) increases as  $t^{1/2}$  after the onset of the pulse. After the maximum magnetic field is reached, the integral splits into two parts. If the expression on the right side of (19) is called  $I(a)$ , the value of  $B$  at later times becomes

$$B = I(a' + a) - I(a') \quad (20)$$

where  $a'$  is the distance by which the minimum in  $u(z')$  is below the lower step of the  $\rho_0'$  pulse in Fig. 1. The first term in (20) increases slowly with  $a'$ , but the second term decreases as  $(a')^{1/2}$  leading to the sharp fall off of the magnetic field after the maximum as shown in Fig. 2.

A complete current pulse may be considered as a linear rise, followed by a constant current, and then a linear decrease. The latter part gives rise to a negative  $\rho'(u)$  and a reversed magnetic field pulse so that the magnetic field for a complete current pulse has the double peaked structure shown in Fig. 2.

### ELECTRIC RADIATION FIELD

In a manner similar to the derivation of (13), the electric radiation field may be found from (2), (8), and (9). The details are omitted, but the result is

$$\vec{E} = - \frac{v}{c_0} \int \left( \frac{\vec{R}}{R} \frac{c}{c_0} - \frac{\vec{v}}{c_0} \right) \frac{1}{R} \rho_0'(u) dz' \quad (21)$$

The direction of  $\vec{E}$  may be determined from the following considerations. If  $\vec{R}$  is assumed approximately constant and denoted by  $\vec{R}_m$  in the region which contributes most strongly to the integral, then

$$\vec{E} \cdot \frac{\vec{R}}{R} = \vec{E} \cdot \frac{\vec{R}_m}{R_m} = I \left( 1 - \frac{v}{c} \cos \theta \right) \quad (22)$$

where  $I$  represents the integral in (21) without the factor in parenthesis and  $\theta$  is the angle between  $\vec{R}_m$  and the  $z$  axis. But the value of  $R_m$  in the region which contributes to the integral is found by evaluating the general expression (21) at  $z' = z_0'$ . To simplify the expression, let the observer be at  $z = 0$  and also assume that the  $\rho_0'$  pulse is centered near  $u = 0$ . Then  $R_m = (s^2 + z'^2)^{1/2}$  may be evaluated using (14) to give

$$R_m = s \left( 1 - \frac{c^2}{v^2} \right)^{-1/2} \quad (23)$$

If the usual Cerenkov angle is defined as  $\cos \theta_c = \frac{c}{v}$   $R_m$  can be written as

$$R_m = \frac{s}{\sin \theta_c} \quad (24)$$

From (22) it is apparent that  $\vec{E}$  is perpendicular to  $\vec{R}_m$  when  $\theta = \theta_c$  and (24) shows that  $\vec{R}_m$  is the value of  $\vec{R}$  at the Cerenkov angle  $\theta_c$ . Thus, the electric field from the front of the pulse (i.e.,  $z' = z_m$ ) is transverse to  $\vec{R}_m$ .

The situation is clarified in Fig. 3. The charge, traveling from left to right, emits a signal from A, which travels to the observer at O, traversing a distance  $R_m$ . The observer is at  $z = 0$  and a distance  $s$  from the path. The field  $\vec{E}$  is perpendicular to  $\vec{R}_m$ . The signal was emitted from A at an earlier time  $t'$  in order to arrive at O at the time  $t$ , with  $c(t-t') = R_m$ . By the time the signal reaches O, the particle is at B, with  $D = v(t-t')$ . Then  $R_m/D = c/v = \cos \theta_c$  as expected.  $D$  is the path length from A to B.

From Fig. 3, one should also note that the field is transverse to  $\vec{R}_m$ , which points from the earlier (retarded time) position of the particle, and is radial relative to the present position of the particle. The former condition holds for typical dipole radiation, while the latter condition holds for the Lienard-Wiechart field for a particle moving with  $v < c$ . The Lienard-Wiechart fields fall off as the inverse square of the distance, and do not represent radiation. In contrast, the

fields discussed here fall off more slowly than  $R^{-1}$  and represent radiation; and the total radiated power is discussed in the next section.



### RADIATED POWER

The energy radiated may be found by calculating the Poynting vector and integrating over a surface. If the surface is a cylinder centered on the z axis, the fields at a given time have a pattern independent of angle and a z dependence as shown in the top curve of Fig. 2. The Poynting vector is, of course, along  $\hat{R}_m$ , and the outward component may be integrated over the cylinder to give the total power radiated. As a crude estimate for the integral, replace the field by the peak field (19) and let the spatial width of the pulse be a. The radiated power is then

$$P(\text{approx}) = \frac{8}{c^2} v I_0^2 \sin^2 \theta_c \quad (25)$$

in cgs units. In the mks system, the square bracket is replaced by  $2\mu_0/\pi$ .

In the earlier calculations,<sup>5,6</sup> the fields and power were expressed in terms of Fourier amplitudes. If the same current pulse is assumed,  $P_\omega$  has frequency components up to the value of  $\omega$  such that the wave length of the radiation is equal to the pulse length. If it is assumed that  $P_\omega$  rises linearly up to this frequency and suddenly drops, the total power radiated becomes (in Mks units)

$$\{P_{\omega} = \frac{\pi}{2} \mu_0 v I_0^2 \sin^2 \theta_c \quad (26)$$

Equations (25) and (26) are both rough estimates and the point is that the similarity of the results is asserted to be confirmation that the calculations in this paper represent the Cerenkov radiation, here expressed in terms of time dependence of the fields.

## DISCUSSION

In preceding sections, the time structure of the electric and magnetic radiation fields was developed. Only the far fields were retained and in the development leading to the B field (13), and the E field (21), only the assumption of a rigid charge confined to a line was introduced. It is seen from these equations that the time derivative of the current is the source function.

The simple model chosen to demonstrate the method of developing the time structures was that of a uniform charge distribution with uniformly varying front and rear sections. This model gives the square pulse charge derivative of height  $\rho'_m$  shown in Fig. 1 which is easy to use in evaluating the integral (13). Similar remarks hold for the power series expansion of  $u(z')$  which is an increasingly better approximation as the time during which the current is changing, decreases. Current variations other than linear may be readily incorporated within the framework given. Also it should be noted that in all cases the variation of  $R^{-2}$  in (13) which was assumed constant in the example will tend to sharpen both the leading and trailing edges of a field pulse.

In the evaluation of the time structure of the fields, the peak field arose when the integral (13) had the most widely spaced limits; a situation which occurs because  $u(z')$  has a negative slope for sufficiently negative values of  $(z' - z)$  as

shown at the left side of Fig. 1. In the non-Cerenkov case ( $\frac{v}{c} < 1$ ) this situation does not arise since then the slope of the  $u(z')$  function always has the same sign. In this case (i.e.  $v < c$ ) the  $u(z')$  curve bends downward instead of upward for large negative values of  $(z' - z)$  and the only contribution to the integral (13) is from small regions of  $z'$ .

These results show how the time structure of Cerenkov radiation arises from the time rate of change of the charge distribution in an electron bunch. Present technology is such that this structure is not observable in the Cerenkov radiation from S or L band Linacs because of their relatively high fundamental frequency. However, induction accelerators with their longer electron bunch structure should produce Cerenkov signals in air for energies greater than about 25 Mev, which should be observable.

The extension of this method of calculation of the fields for both Cerenkov and sub-Cerenkov charge velocities is easily made for cases for which the charge derivative  $\rho'(u)$  is not constant. A detailed report is under preparation.

Finally, we note that although the results of other workers<sup>4,7</sup> often have singularities in the radiated power at the Cerenkov angle, the present results and our previous ones<sup>5,6</sup> show that the radiated power is finite whether calculated in the frequency or time domain. Also it should be noted that causality is satisfied because the fields are zero at times earlier than the leading edge of the pulse shown in Fig. 2.

### ACKNOWLEDGEMENTS

This work was supported by the U.S. Naval Postgraduate School Foundation Research Program and the Naval Surface Weapon Center, White Oak, Maryland.

### REFERENCES

1. P. Čerenkov, Dokl. Akad. Nauk. SSSR 2 451 (1934).
2. I. M. Frank and I. Tamm, Dokl. Akad. Nauk. SSSR 14 107 (1937).
3. J. V. Jelley, "Čerenkov Radiation and Its Applications" (Pergamon, London, 1958).
4. V. P. Zrelov, "Čerenkov Radiation in High Energy Physics", (Atomizdat, Moscow, (1968); translation: Israel Program for Scientific Translations, Jerusalem, (1970)).
5. F. R. Buskirk and J. R. Neighbours, Phys. Rev. A 28, 1531 (1983).
6. J. R. Neighbours and F. R. Buskirk (To be published in Phys. Rev. A 29, June (1984)).
7. I. Tamm, J. Phys SSSR 1 439 (1939).

### FIGURE CAPTIONS

Figure 1. The function  $u = z' - vt'$ , defined in the text is plotted for increasing times  $t_1, t_2, t_3$  at the point of observation. The corresponding current derivative profile, on the right, is a function of  $u$  only and remains fixed in time. The field signal pulse starts at  $t_2$ , and reaches a maximum at  $t_3$ .

Figure 2. The electric field pulse generated by the beam current profile, shown in the lower curve.

Figure 3. Geometrical relations for the Cerenkov pulse. The source ( $\rho_0'$ ) at A emits a signal at an early time giving the  $\vec{E}$  field at the observer 9; when the field reaches the observer, the particle is at B.

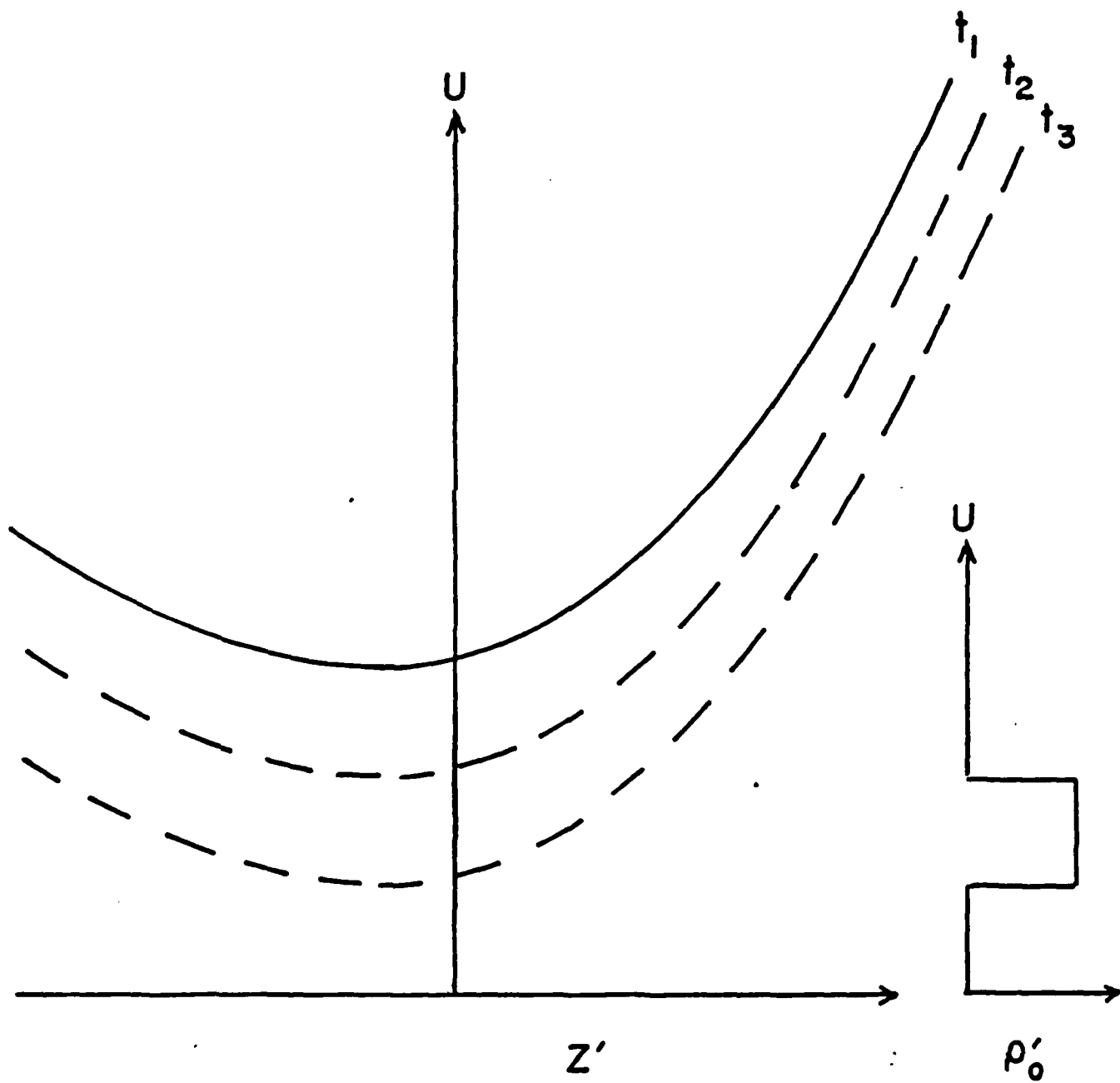


Figure 1.



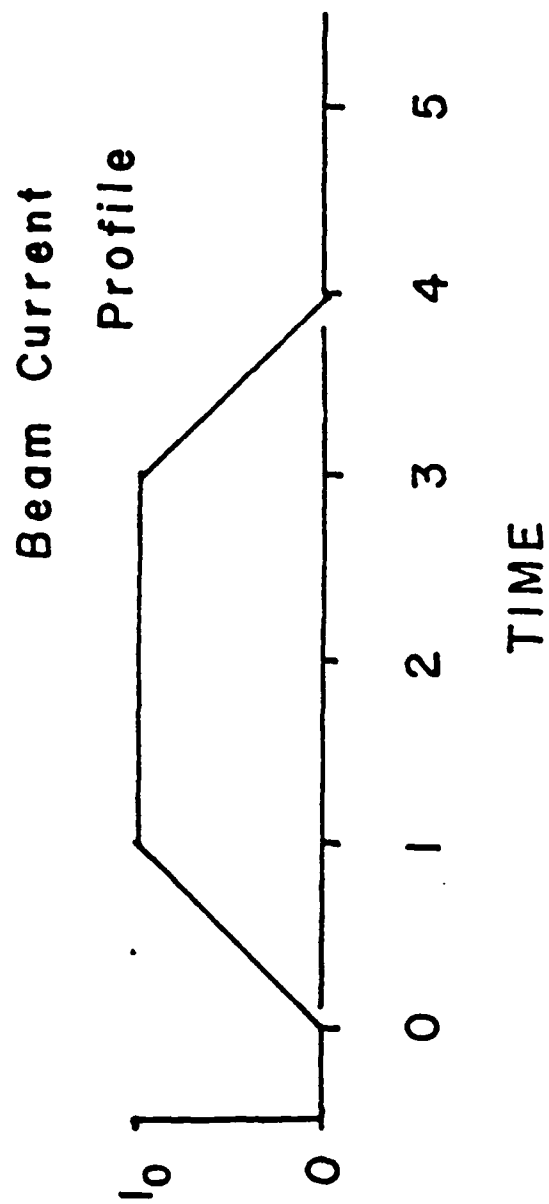
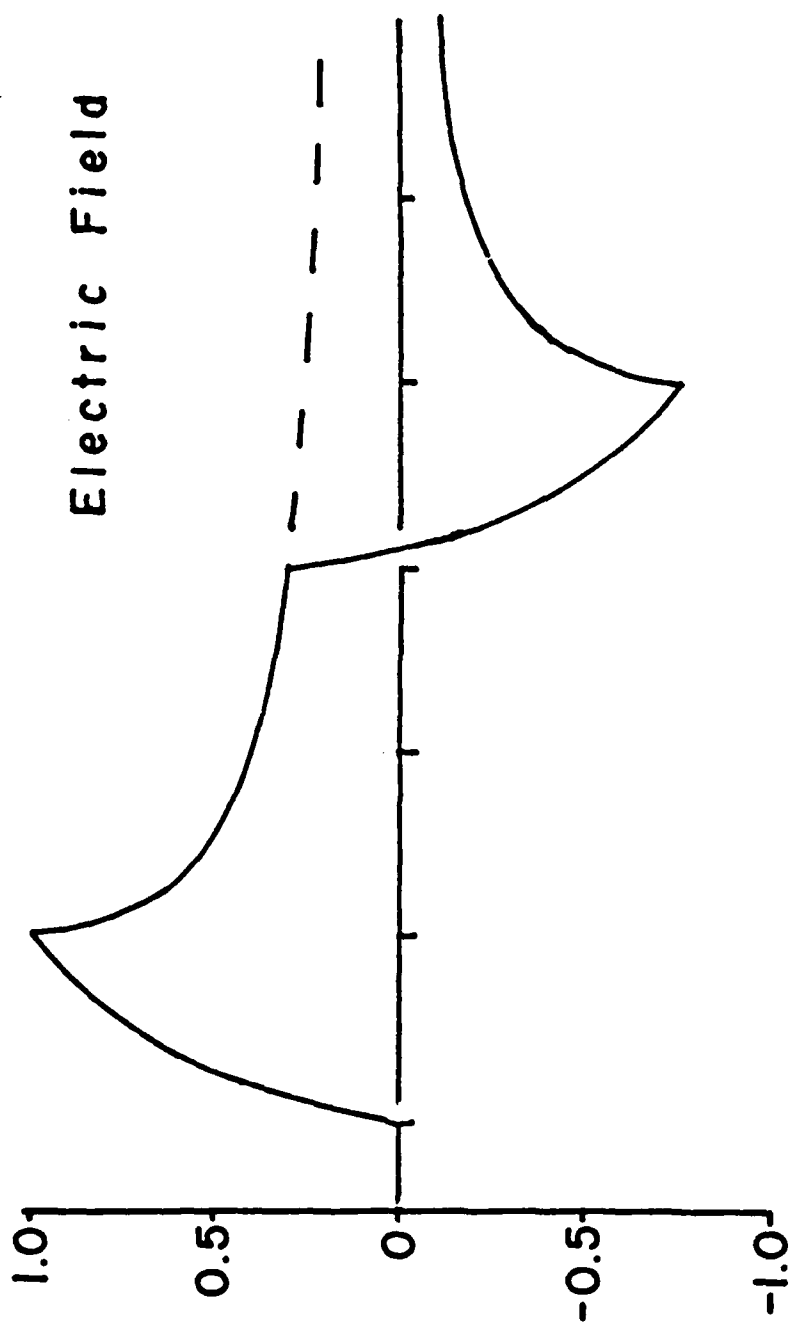


Figure 2.

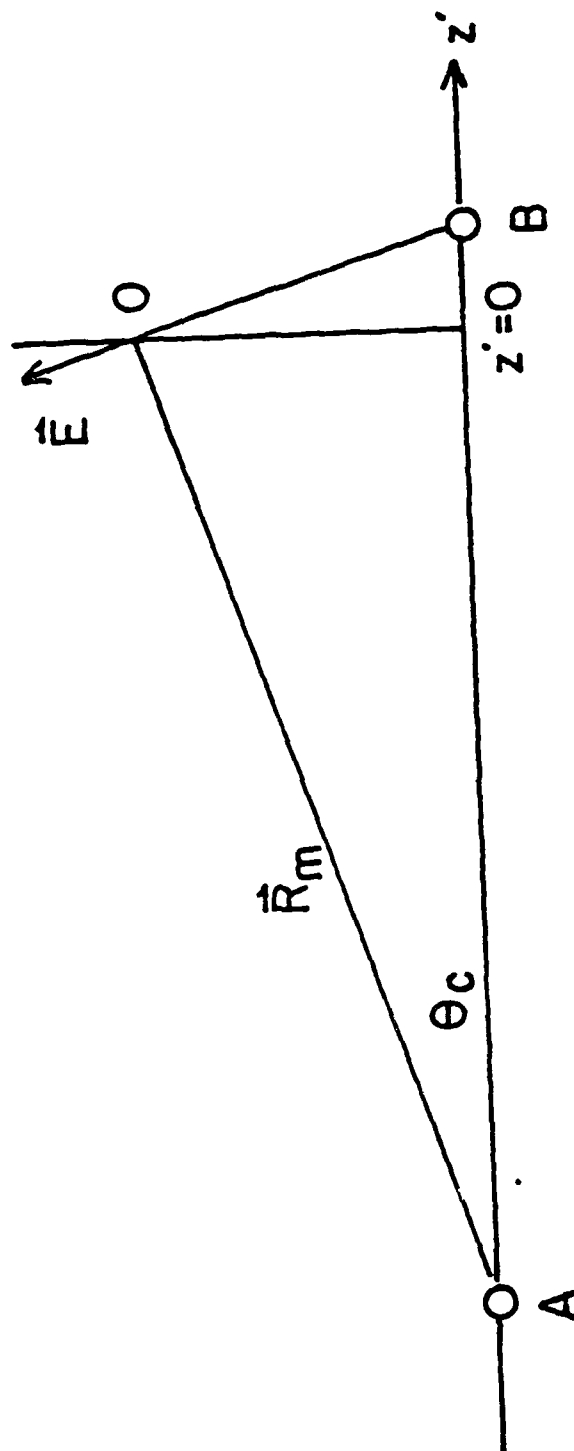


Figure 3.

# DISTRIBUTION LIST

Office of Naval Research CDR R. Swafford 800 N. Quincy Street Arlington, VA 22217	1
Office of Naval Research CDR James Offutt 1030 East Green Street Pasadena, CA 91106	1
Library Code 0142 Naval Postgraduate School Monterey, CA 93943	2
Office of Research Administration Code 012A Naval Postgraduate School Monterey, CA 93943	2
F. R. Buskirk & J. R. Neighhours Naval Postgraduate School Physics Department, Code 61 Monterey, CA 93943	20
Dr. Thomas Starke M4, M.S. P942 Los Alamos National Laboratory Los Alamos, NM 87545	1
MAJ E. W. Pogue M4, M.S. P942 Los Alamos National Laboratory Los Alamos, NM 87545	1
Dr. Charles Bowman D442 Los Alamos National Laboratory Los Alamos, NM 87545	1
Dr. Thomas Fessenden L-436 Lawrence Livermore National Laboratory Box 808 Livermore, CA 94550	1

Dr. Richard Briggs L-321 Lawrence Livermore National Laboratory Box 808 Livermore, CA 94550	2
Dr. C. M. Huddleston R-401 Naval Surface Weapons Center White Oak Silver Spring, MD 20910	3
CAPT R. L. Topping PMS 405 Strategic Systems Project Office Naval Sea Systems Command Washington, D.C. 20376	1
Dr. David Merritt PMS 405 Strategic Systems Project Office Naval Sea Systems Command Washington, D.C. 20376	1
CDR William Bassett PMS 405 Strategic Systems Project Office Naval Sea Systems Command Washington, D.C. 20376	1
Director, Defense Advanced Research Project Agency ATTN: LCOL Richard A. Gullickson 1400 Wilson Blvd. Arlington, VA 22209	2
Defense Technical Information Center Cameron Station Alexandria, Virginia 22314	2